Journal of King Saud University – Science 32 (2020) 1444–1450

Contents lists available at ScienceDirect

Journal of King Saud University – Science

journal homepage: www.sciencedirect.com

Original article

A facile approach to develop industrial waste encapsulated cryogenic alginate beads to sequester toxic bivalent heavy metals

Ayoub Abdullah Alqadami [a], Moonis Ali Khan [a,*], Masoom Raza Siddiqui [a], Zeid Abdullah Alothman [a], Sadia Sumbul [b]

[a] Chemistry Department, College of Science, King Saud University, Riyadh 11451, Saudi Arabia
[b] Department of Chemistry, College of Science, Princess Noura Bint Abdul Rehman University, Riyadh, Saudi Arabia

ARTICLE INFO

Article history:
Received 19 September 2019
Revised 27 October 2019
Accepted 26 November 2019
Available online 5 December 2019

Keywords:
Waste management
Silico-manganese fumes
Cryogenic beads
Heavy metals
Adsorption

ABSTRACT

Herein, a solid industrial waste management approach converting silico-manganese fumes (SMF) waste to SMF impregnated cryogenic alginate beads (SMFCAB) and its applicability to remove potentially toxic cadmium Cd(II) and lead Pb(II) was proposed. Infra-red, elemental, and XPS analysis data supported the formation SMFCAB. Morphologically, pristine SMFCAB surface was synonymous to cauliflower with agglomerated and interconnected particles. The respective XPS spectral peaks for Cd(II) and Pb(II) at 408 and 144.5 eV binding energies confirmed their adsorption on SMFCAB. The adsorption was pH dependent, with maximum uptakes at pH: 5.5 (for Pb(II)) and 7.2 (for Cd(II)). Contact time studies depicts comparatively rapid Pb(II) adsorption, accomplishing 72% adsorption in 10 min, while only 50% Cd(II) adsorption was accomplished within same time slot. The adsorption data at varied temperatures was fitted to Freundlich isotherm model, while kinetics data was fitted to pseudo-second-order model. Exothermic adsorption process with maximum monolayer adsorption capacities (q_m) on SMFCAB were 200 mg/g (for Pb(II)) and 178.6 (for Cd(II)) at 298 K. Hydrochloric acid (0.01 M) eluted maximum amount of metal ions.

1. Introduction

Cadmium Cd(II) and lead Pb(II) are among the potentially toxic heavy metals (Rao et al., 2011; Jalees et al., 2019). They are non-degradable, carcinogenic and can impair human's renal, hepatic, reproductive and nervous systems (Alakhras, 2019). Therefore, detection, determination, and thereafter diminishing their concentrations below permissible levels is a vital step towards safeguarding flora and fauna. The allowable limits for Pb(II) and Cd(II) in drinking water, reported by World Health Organization (WHO) were 0.010 and 0.005 mg/L, respectively (Ajmal et al., 2006; Teoh et al., 2013). The respective permissible limits for Pb(II) and Cd (II) in drinking water set by SASO, a local regulatory authority were 0.010 and 0.003 mg/L (Aldawsari et al., 2017).The effluents discharge from mining, fertilizer, paint, electroplating, battery industries contains higher levels of Pb(II) and Cd(II) (Khan et al., 2019a). Therefore, these metals should be removed from aforementioned effluents prior to their discharge in surface and sub-surface water.

Membrane filtration, chemical precipitation, adsorption, and ion-exchange processes have been engineered to sequester heavy metals from water. Adsorption is a most favorable water remediation process among them as it is facile, cost effective, and selective. 3-aminopropyl trimethoxy silane-modified kaolinite (Fatimah, 2018), *Acacia senegal* (L.) pods activated carbon (Adetokun et al., 2019), polymers with bicomponent polymer brushes (Luo et al., 2017), and CCM (Teoh et al., 2013) have been used to abate Cd (II) and Pb(II) from water. Effectiveness of natural polymers viz. sodium alginate (SA) and chitosan in the removal of pollutants have also been studied (Lee et al., 2017; Farooghi et al., 2018). Among them, SA is a non-toxic and cost effective polysaccharide extracted from brown seaweeds (Garmia et al., 2018; Lee et al., 2017). Sodium alginate can be easily transformed to composite beads by encapsulation for water remediation applications (Pawar et al., 2018). Khan et al. developed nano-graphite encapsulated beads to remove Co(II) and Mn(II). About 80–92% metals

* Corresponding author.
E-mail address: mokhan@ksu.edu.sa (M.A. Khan).

Peer review under responsibility of King Saud University.

Production and hosting by Elsevier

https://doi.org/10.1016/j.jksus.2019.11.040
1018-3647/

adsorption was accomplished within 4 h at pH: 8 (Khan et al., 2014). Abas et al. developed composite beads using mangrove and alginate for Pb(II) ions sequestering from water with an excellent removal efficiency of about 99% (Abas et al., 2015). About 73.7% of Cd(II) adsorption was observed on cross-linked chitosan/PVA beads at pH: 6 (Farooghi et al., 2018). Phosphate embedded beads were used for Pb(II) and Cd(II) removal from single-metal system with 263.2 and 82.6 mg/g as their respective adsorptive capacities (Wang et al., 2016). The efficacy of iron oxide modified clay-activated carbon composite beads were tested for Pb(II) and Cd(II) removal from water with 74.2 and 41.3 mg/g uptake capacity at 25 °C, respectively (Pawar et al., 2018). The anionic surfactant bilayer anchored chitosan beads were tested in Pb(II) removal (Pal and Pal, 2017).

Herein, silico-manganese fumes (SMF) waste, generated during low-carbon steel production operation in a basic oxygen furnace was used to develop beads by encapsulating SMF into SA. It is chemically composed of 18% silica and 56% manganese along with traces of other elements such as iron, and calcium. Conventionally, SMF is used in building of roads, for sintering and as a raw material for making cement. To skip the usage of toxic and high-priced cross-linker for withholding structural geometry, developed beads were lyophilized to obtain SMF impregnated cryogenic alginate beads (SMFCAB). The SMFCAB was characterized by using state-of-art characterization tools. The efficacy of SMFCAB as an adsorbent was tested in the removal of potentially toxic bivalent Pb(II) and Cd(II) from water through batch scale experiments. The reusability of SMFCAB was also tested.

2. Experimental

2.1. Chemicals and reagents

Nitrate salts of cadmium [$Cd(NO_3)_2{\cdot}4H_2O$, BDH, England] and lead [$Pb(NO_3)_2$, BDH, England] were used to prepare the stock solutions of model adsorbates. Sodium alginate (SA: $C_6H_9NaO_7$, Sigma-Aldrich, USA), calcium chloride ($CaCl_2$: Sigma-Aldrich, USA) and sodium hydroxide (NaOH: Sigma-Aldrich, USA) were utilized for the synthesis of SMFCAB. Hydrochloric acid (HCl: Merck, Germany), nitric acid (HNO_3: Merck, Germany), and sulfuric acid (H_2SO_4: Merck, Germany) were used to desorb heavy metal ions from SMFCAB. The analytical reagent (A.R) grade chemical and reagents were used throughout the research.

2.2. Synthesis of SMFCAB

Silico-manganese fumes waste (25 g, Jubail, Saudi Arabia) was taken in 100 mL beaker, repeatedly rinsed with deionized (D.I) water to remove unsettled dust particles. Thereafter, waste was overnight dried at 60 °C. Sodium alginate (2%) was solubilized in 12.5 mL 0.1 M NaOH solution. Thereafter, SMF waste (2 g) under continuous magnetic stirring at 120 rpm was suspended into it. The suspension was continuously stirred for 2 h. 500 mL calcium bath (0.1 M $CaCl_2$ solution) was prepared, cooled to 5 °C in a refrigerator. The homogenized SMF/SA suspension was loaded in a clinical syringe (5 mL). The syringe was inserted into a syringe pump operated at 5 mL/min flow rate to avoid sedimentation. The beads were dropped from 6 cm height into a cooled calcium bath to form spherical SMF impregnated alginate beads of uniform size, aged for 48 h in a calcium bath. Thereafter, the beads were lyophilized (VirTis Bench Top Pro with Omnitronics™) to prepare cryogenic SMF impregnated alginate beads, nomenclature as "SMFCAB" hereafter. Scheme 1 illustrates the development of SMFCAB.

2.3. Characterization of SMFCAB

The IR spectra of the samples were recorded by Fourier transform infrared (FT-IR) spectrometry (Nicolet 6700, Thermo Scientific, USA). The surface morphology of SMFCAB samples was examined by scanning electron microscopy (SEM; Nova 200 Nano-Lab, FEI). Elemental composition of SMFCAB samples was determined by energy dispersive X-ray (EDX) spectroscopy (AMETEK Nova 200). The surface elemental composition of pristine and metals saturated SMFCAB was evaluated by X-ray photoelectron spectroscopy (XPS: Joel JPS-9200). Zeta potential (ζ) analyzer (Nano Plus Series, Particulate Systems, USA) was used to estimate the isoelectric point (IEP) of SMFCAB sample.

2.4. Adsorption and desorption experiments

The batch scale experiments were carried out in laboratory to study heavy metals adsorption and desorption on SMFCAB. Adsorbate (Cd(II)/Pb(II)) solution (25 mL) of C_o: 25 mg/L was treated for 24 h at 100 rpm with 0.01 g SMFCAB under room temperature conditions. After 24 h, both adsorbate/adsorbent were separated. The residual adsorbate concentration was analyzed by atomic absorption spectrometer (AAS: Perkin Elmer, PinAAcle™ 900 T). The equilibrium uptake capacity (q_e) and adsorption (%) of adsorbate were determined as:

$$q_e(\mathrm{mg/g}) = (C_o - C_e) \times \frac{\mathrm{V}}{\mathrm{m}} \tag{1}$$

$$\mathrm{Adsorption}(\%) = \frac{C_o - C_e}{C_o} \times 100 \tag{2}$$

where C_o and C_e are the initial and equilibrium concentrations of heavy metal solution, respectively, V is the volume of heavy metal solution, and m is the mass of SMFCAB.

Effect of experimental parameters viz. adsorbate concentration (C_o: 25–300 mg/L), adsorbent concentration (m: 0.01–0.05 g), temperature (T: 298–318 K), contact time (t: 1–1440 min), initial pH (pH_i: 1.78–10.12) on adsorption was studied.

The adsorbed heavy metal ions were eluted from saturated SMFCAB samples during desorption experiments using strong acids (HCl, HNO_3, and H_2SO_4) solutions of 0.01 M concentrations. Briefly, 0.01 g of SMFCAB was equilibrated with 25 mL heavy metal solution of C_o: 25 mg/L for 24 h over a shaker incubator at 100 rpm and T: 298 K. At equilibrium, SMFCAB was separated and washed with D.I water to remove unadsorbed traces of metal ions. Thereafter, heavy metal saturated SMFCAB was treated with 25 mL 0.01 M HCl to elute heavy metal ions. Similar procedure was adopted with 0.1 M HNO_3 and 0.1 M H_2SO_4 eluent solutions. Desorption (%) was calculated as:

$$\mathrm{Desorption}(\%) = \frac{\mathrm{Concentration\,of\,adsorbate\,desorbed\,by\,eluent}}{\mathrm{Concentration\,of\,adsorbate\,adsorbed\,on\,SMFCAB}} \times 100 \tag{3}$$

3. Results and discussion

3.1. Characterization of SMFCAB

Fig. 1a showed the FT-IR spectra of SA and SMFCAB (before and after Cd(II) and Pb(II) adsorption). A band at 3449 cm^{-1} associated with hydroxyl (–OH) group vibrations was exhibited by SA spectrum. Two side by side bands at 2850 and 2924 cm^{-1} displayed aliphatic C–H symmetric and asymmetric stretching (Saha and Ray, 2013). Weak band at 1730 cm^{-1} was due to free carboxyl groups

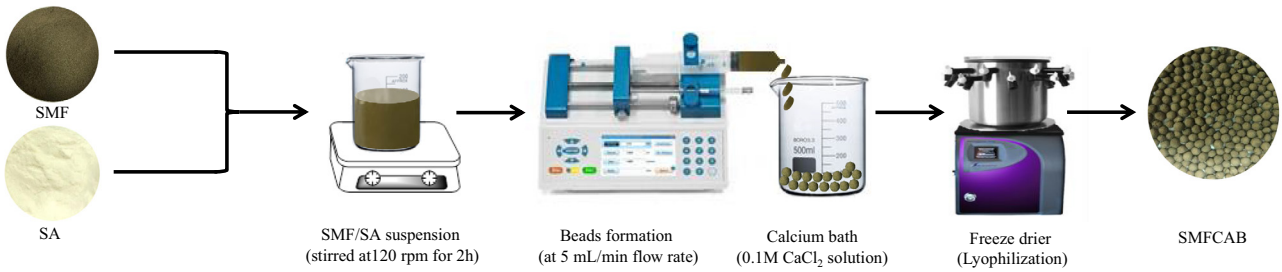

Scheme 1. Schematic illustration of SMFCAB development.

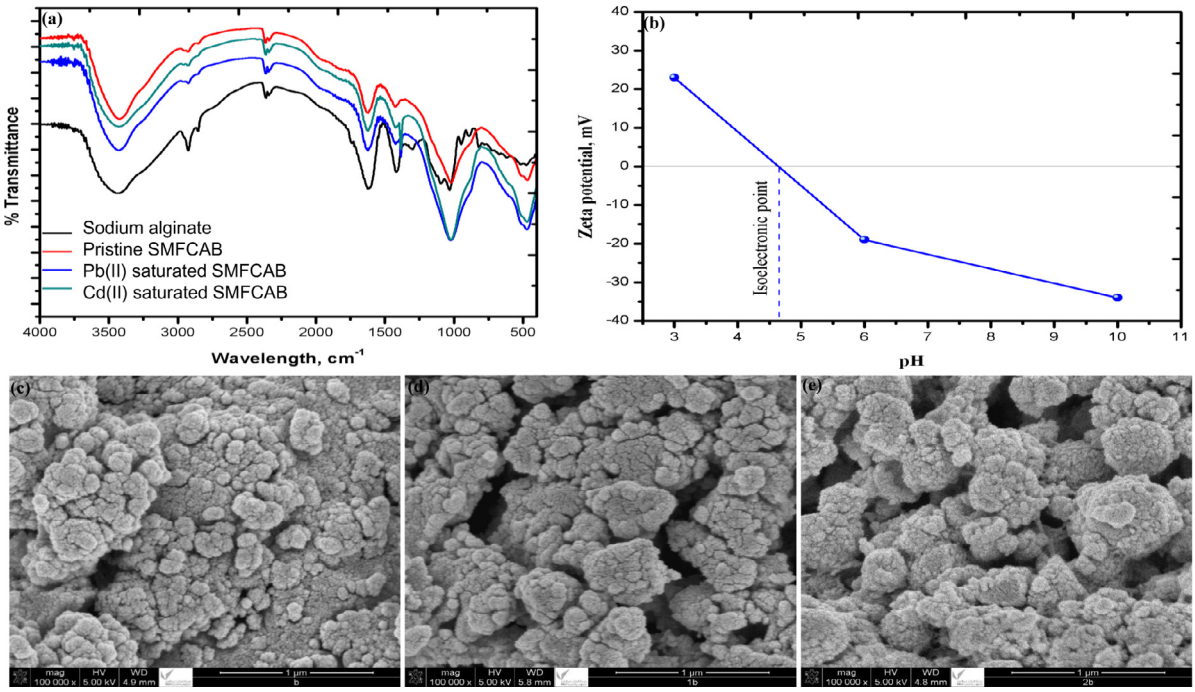

Fig. 1. FT-IR spectra (a), Zeta potential plot (b), SEM images of pristine (c), Cd(II) saturated (d), and Pb(II) saturated (e) SMFCAB.

of SA. The bands at 1612, 1412, 1092 and 1031 cm^{-1} were attributed to carboxylate group's asymmetric, symmetric stretching vibrations, stretching vibrations of the C—O and C—O—C bonds, respectively (Voo et al., 2015). Bands shifting, and hiding (present in SA spectra) and reappearance of new bands was observed in FT-IR spectra of SMFCAB. Band at 3449 cm^{-1} (for —OH group) moved to 3424 cm^{-1}. Bands at 2924 and 2850 cm^{-1} were shuffled to 2934 and 2859 cm^{-1} with reduced intensities. A strong band associated with the presence of metal oxide appeared at 467 cm^{-1} in SMFCAB spectrum, confirming the presence of metal oxide in SMF waste. Band at 1032 cm^{-1} relocated to 1016 cm^{-1} in SMFCAB spectrum. Cd(II) and Pb(II) ions saturated SMFCAB spectra showed shifting and a decrease in band intensity at 1419 to 1422 cm^{-1}. The sharp bands with a slight shift in positions from1016 and 467 cm^{-1} to1022 and 474 cm^{-1} appear in heavy metals saturated SMFCAB.

The zeta potential (z) plot of SMFCAB is illustrated in Fig. 1b. The magnitude of z for studied pH range: 3 – 10 varied between 23 and −34 mV. The isoelectric point (IEP) for SMFCAB was at ~4.6. Thus, SMFCAB surface was positively charge below IEP and negatively charged above IEP. Morphological analysis of pristine SMFCAB showed uneven surface, structurally synonymous to cauliflower with irregular size agglomerated and interconnected particles (Fig. 1c). After heavy metals adsorption, the size of agglomerated structures increases. Additionally, some cracks were appeared over metals saturated SMFCAB, owing to diffusion of adsorbate ions during the adsorption (Fig. 1d and e). Elemental analysis data and plots showed the presence of Si and Mn in SMFCAB (Fig. S1a). Also, the elemental Na of SA (used to encapsulate SMF) and elemental Ca of $CaCl_2$ (used as calcium bath to form beads) were present. Fig. S1 (b and c) illustrates the presence of heavy metal ions over SMFCAB surface, confirming their adsorption over SMFCAB.

The peaks at 532, 348, 284.7, 202, 155, 109.9, 52, 34, and 711 eV corresponds to O 1 s, Ca 2p, C 1 s, Cl 2p, Si 2p, Al 2 s, Mn 3p, Na 2p and Fe 2p, respectively (Rauf et al., 2017; Ilton et al., 2016) were observed in XPS spectra of pristine SMFCAB (Fig. 2). Among them, the three peaks, corresponding to O 1s, C 1s, and Na 2p were for SA, while other peaks were due to SMF waste encapsulated in SA beads. The saturated SMFCAB samples showed peaks for Cd 3d and Pb 4f at 408 and 144.5 eV (Chen et al., 2017), respectively, confirming their adsorption of on SMFCAB.

3.2. Adsorption studies

As illustrated in Fig. 3a Pb(II) and Cd(II) uptake on SMFCAB increases with a rise in initial pH (pH_i). For Pb(II), adsorptive removal increases in pH_i range: 1.8–5.5, while for Cd(II) removal was found to increase in pHi range: 2.3–7.2. At lower pHi, the num-

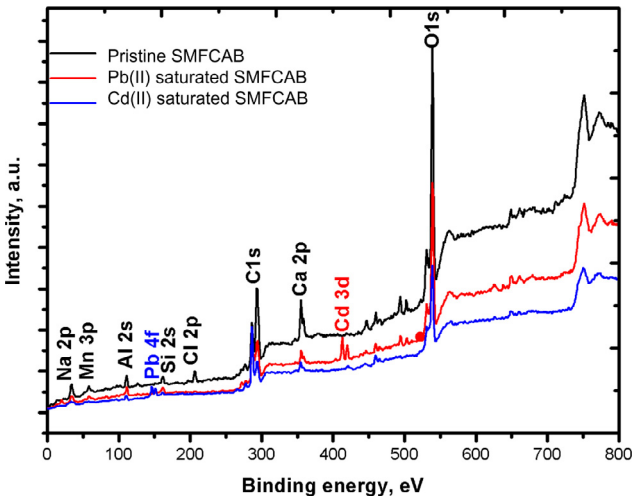

Fig. 2. XPS spectrum of SMFCAB.

ber of hydronium (H_3O^+) ions exceeds in solution resulting a competition with cationic metal ions to occupy SMFCAB surface (Khan et al., 2019a). Thus, Pb(II) and Cd(II) uptake on SMFCAB at lower pHi values was very less. The respective maximum q_e of Pb(II) and Cd(II) (C_o: 25 mg/L) were 57.29 and 59.9 mg/g at pHi: 5.5 and 7.2. Further increase in pHi for both heavy metal solutions results a decrease in their respective removal. Metal ions hydrolysis might be a possible reason behind a decrease in adsorption. Nearer pH values were observed for Pb(II) (Pal and Pal, 2017) and Cd(II) (Bhunia et al., 2018) adsorption during previous studies.

The contact time plots showed rapid initial uptake of Pb(II) on SMFCAB accomplishing 72% adsorption in 10 min, while for Cd (II) the uptake was comparatively slow and only 50% Cd(II) adsorption was accomplished in 10 min (Fig. 3b). Comparatively smaller hydrated radii of Pb(II) is a probably responsible for its rapid uptake. The respective equilibration time for Pb(II) and Cd(II) removal were 90 and 120 min, comparatively better than previous studies (Pawar et al., 2018; Fu et al., 2016; Bohli et al., 2015). Uptake capacities of Pb(II) and Cd(II) at equilibrium were 60.3 and 56.2 mg/g, respectively.

Influence of SMFCAB concentration on heavy metals adsorption was assessed in range: 0.01–0.05 g. Fig. 3c showed a drop in Pb(II) removal from 57 to12 mg/g, while %uptake increases from 91 to 94% with an increase in SMFCAB concentration. Likewise, for Cd (II), as illustrated in Fig. 3d the removal capacity decreases from 55 to 11.5 mg/g, while %adsorption increases from 87.6 to 93.6% for aforesaid SMFCAB concentration. The higher concentration of SMFCAB offers greater number of active binding sites which led to enhanced sequestration of metals (Pal and Pal, 2017).

Effect of initial concentrations (C_o: 25–300 mg/L) on heavy metals adsorption onto SMFCAB was evaluated at varied temperatures (T: 298–318 K) (Fig. 4 a and b). At 298 K, Pb(II) adsorption increases from 58 to 248 mg/g, while for Cd(II), the removal increases from 26 to 102 mg/g, respectively. Higher concentration of metal ions provides superior driving force to diffuse into SMFCAB surface. Also, at higher metal ions concentration the collisions between metal ions and active binding sites present on SMFCAB surface increases, finally resulting in higher metal uptake (Khan et al., 2019b). On the other hand, the metal ions uptake on SMFCAB deceases with a rise in temperature depicting exothermic adsorption on SMFCAB, similar to previous results (Aldawsari et al., 2017).

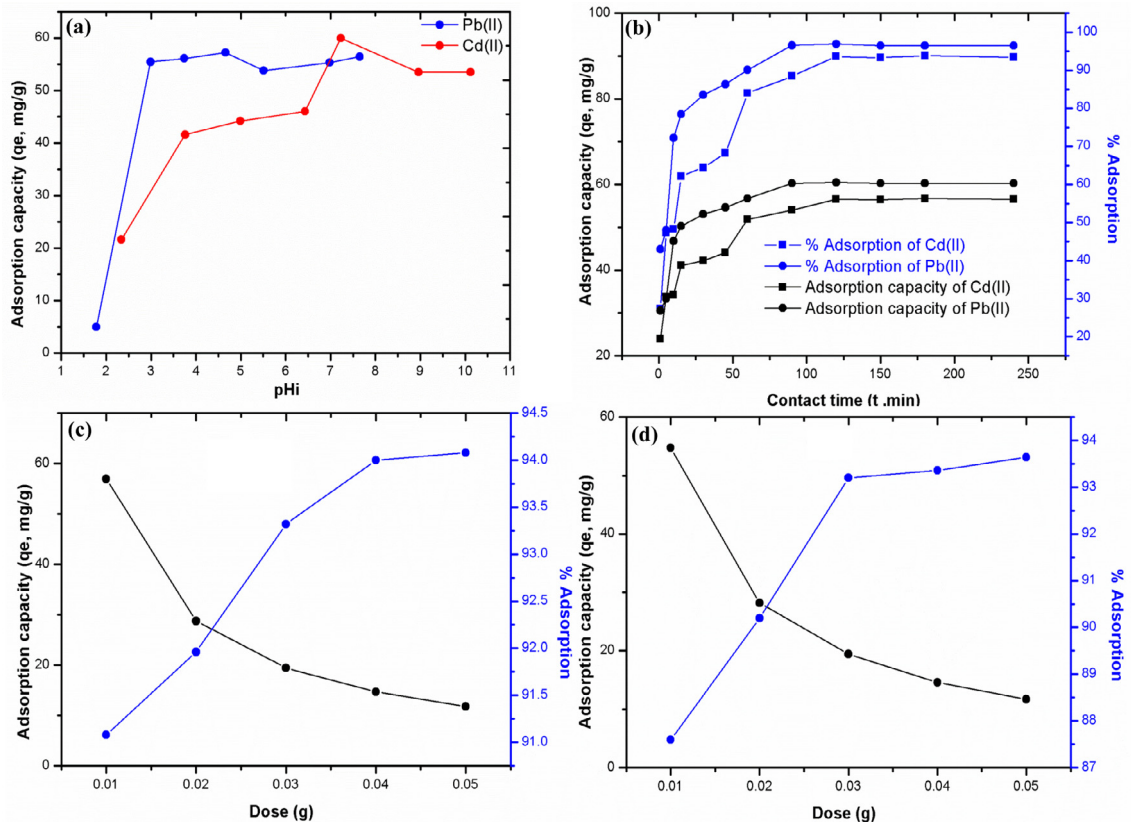

Fig. 3. pH (a), contact time (b) plots for heavy metals adsorption on SMFCAB, SMFCAB concentration plots for Pb(II) (c), and Cd(II) (d) adsorption. (Experimental conditions: C_o: 25 mg/L; m: 0.01 g (for pH and contact time study); agitation speed: 100 rpm; V: 0. 025 mL; T: 298 K; contact time: 24 h (for pH and SMFCAB concentration study).

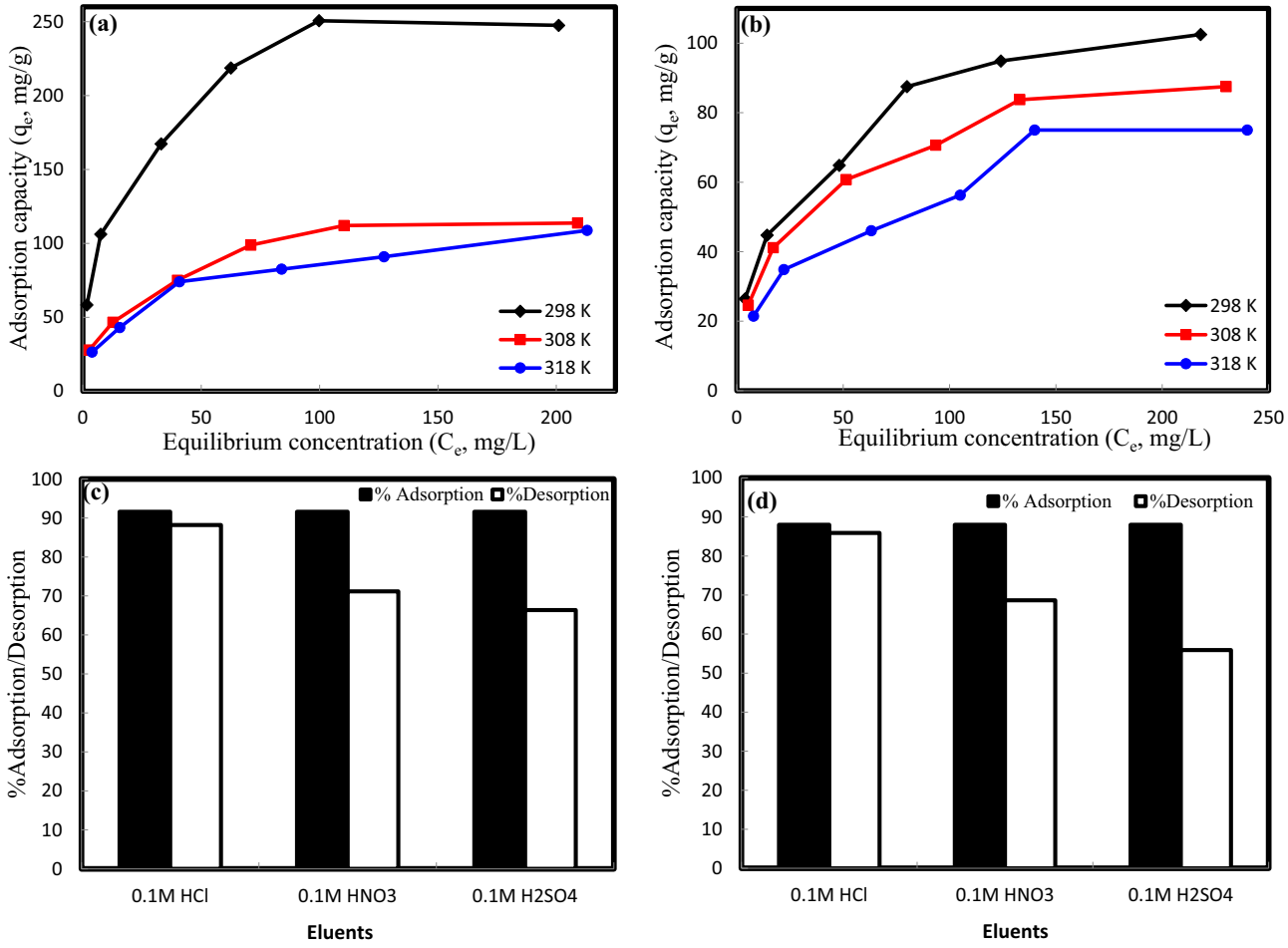

Fig. 4. Effect of initial concentrations on Pb(II) (a) and Cd(II) (b) adsorption onto SMFCAB, desorption plots of Pb(II) (c), and Cd(II) (d) from SMFCAB. (Experimental conditions: *m*: 0.01 g; agitation speed: 100 rpm; V: 0. 025 mL; contact time: 24 h , C_o: 25 mg/L (for desorption study)).

3.3. Adsorption modeling

3.3.1. Adsorption isotherms

The two-parameters Langmuir (Langmuir, 1918) and Freundlich (Freundlich, 1906) isotherm models (details in Text S1 and data presented in Table 1) were fitted to adsorption data. Comparatively greater regression coefficient (R^2) values of Freundlich model for both metals adsorption on SMFCAB at studied temperatures supported the fitting of model. Thus, it could be concluded that Pb (II) and Cd(II) adsorption on SMFCAB surface was heterogeneous, in line with previous research (Alsohaimi et al., 2015). The process favorability was further supported by Freundlich constant *n* values ($n > 1$). Freundlich constant (K_f) values at varied temperatures decreases with a rise in temperature this means significant adsorption at lower temperature. The respective maximum monolayer uptake capacities (q_m) for Pb(II) and Cd(II) adsorption on SMFCAB were 200 and 178.6 mg/g at 298 K, comparatively higher than previous studies (Table S1) (Pal and Pal, 2017; Bhunia et al., 2018; Ngah and Fatinathan, 2010; Tran et al., 2010; Feng et al., 2017; Sahraei et al., 2017).

3.3.2. Adsorption kinetics

The data for heavy metals adsorption on SMFCAB was fitted to Lagergren-first-order (Lagergren, 1898) and pseudo-second-order (Ho and McKay, 1998) kinetic models. Supplementary information (Text S2) furnished models details. As illustrated in Table 2, the R^2 values of pseudo-second-order model were comparatively higher (nearer to unity) than pseudo-first-order model, confirming its applicability for Pb(II) and Cd(II) adsorption on SMFCAB. Fitting of the model to kinetic data was further supported by closer $q_{e,cal.}$ and $q_{e,\ exp.}$ values. The observed results agreed well with previously reported results (Aldawsari et al., 2017; Alqadami et al., 2018a).

3.3.3. Adsorption thermodynamics

Gibbs free energy change (ΔG°), standard enthalpy change (ΔH°), and standard entropy change (ΔS°) parameters were calculated. Supplementary information (Text S3) furnished over all details. Table 3 presents thermodynamics data. Magnitudes of ΔH° for both Pb(II) and Cd(II) adsorption on SMFCAB at varied initial concentrations were negative, confirming exothermic process, in line with earlier study (Bhunia et al., 2018). The spontaneous process was affirmed by the negative magnitudes of ΔG°. Higher negative value for ΔG° at 25 °C (lower temperature) indicates more favored adsorption process. The negative ΔS° values indicate randomness at solid/solution interface. Similar result was observed for Pb(II) removal (Pal and Pal, 2017).

3.4. Desorption studies

Batch mode desorption experiments were conducted. As shown in Fig. 4(c and d), Pb(II) and Cd(II) elution from saturated SMFCAB was 88 and 86% (maximum) with 0.01 M HCl, respectively followed by 0.01 M HNO_3(with 71% Pb(II) and 68% Cd(II) recovery) and 0.01 M H_2SO_4 (with 66% Pb(II) and 56% Cd(II) recovery).

Table 1
Isotherm parameters for Pb(II) and Cd(II) adsorption on SMFCAB.

Metal ions	Temperature (K)	Isotherm models						
		Langmuir				Freundlich		
		q_m (mg/g)	b (L/mg)	R_L	R^2	K_f (mg/g)(L/mg)$^{1/n}$	n	R^2
Pb(II)	298	200.0	0.350	0.103	0.923	58.5	3.35	0.979
	308	192.3	0.147	0.254	0.925	40.2	2.86	0.977
	318	178.6	0.104	0.325	0.942	33.7	2.81	0.978
Cd(II)	298	178.6	0.105	0.323	0.957	34.3	2.86	0.984
	308	161.3	0.080	0.385	0.976	29.4	2.90	0.982
	318	137.0	0.056	0.471	0.961	20.5	2.66	0.972

Table 2
Kinetic parameters for the adsorption of Pb(II) and Cd(II) on SMFCAB.

Metal ions	C_o (mg/L)	$q_{e,\ exp.}$ (mg/g)	Kinetic models					
			Pseudo-first-order			Pseudo-second-order		
			$q_{e,\ cal.}$ (mg/g)	K_1 (1/min)	R^2	$q_{e,\ cal.}$ (mg/g)	K_2 (g/mg-min)	R^2
Pb(II)	25	60.31	35.59	0.049	0.904	61.72	0.004	0.999
Cd(II)	25	56.31	32.95	0.026	0.947	58.47	0.002	0.997

Table 3
Thermodynamic parameters for the adsorption of Pb(II) and Cd(II) on SMFCAB.

Metal ions	C_o (mg/L)	$-\Delta H°$ (KJ/mol)	$-\Delta S°$ (J/mol·K)	$-\Delta G°$ (KJ/mol)		
				298 K	308 K	318 K
Pb(II)	50	36.92	109.83	4.28	2.89	2.09
	100	13.09	38.19	1.75	1.26	0.99
	200	12.18	38.21	0.83	0.35	0.07
Cd(II)	50	27.23	83.46	2.28	1.67	0.61
	100	32.12	105.25	0.69	0.14	1.43
	200	14.02	51.15	1.21	1.75	2.24

Maximum recovery with 0.01 M HCl solution might be due to the relatively smallest ionic size of chloride ion (Cl^-) than sulfate (SO_4^{2-}) and nitrate (NO_3^-) ions. The results were in line with previously reported works on mesoporous amide citric anhydride metal organic framework (Alqadami et al., 2018b), and magnetic bone biochar (Alqadami et al., 2018a).

4. Conclusions

In conclusion, present work successfully reported the conversion of SMF (steel industry waste) to SMFCAB and its utilization to sequester potentially toxic bivalent heavy metals. The studied experimental parameters have a sound impact on Pb(II) and Cd (II) adsorption. Pb(II) uptake was comparatively higher and rapid than Cd(II). The magnitudes of q_m for Pb(II) and Cd(II) adsorption on SMFCAB at 298 K were 200 and 178.6 mg/g, respectively. Adsorption kinetics data was fitted to pseudo-second-order model. Thermodynamically, the process was favored at lower temperature. 88 to 86% heavy metal ions were recovered from SMFCAB by 0.01 M HCl. Hence, it could be inferred that conversion of SMF to SMFCAB and its environmental remediation applications is an ecological and economical alternate step towards steel industry waste management.

Funding

The reported research was conducted through funding provided to Dr. Moonis Ali Khan (corresponding author) by DSR, KSU through Research Group No. RG-1437-031. The authors declare that they have no conflict of interest.

Declaration of Competing Interest

The authors declare that they have no known competing financial interests or personal relationships that could have appeared to influence the work reported in this paper.

Acknowledgement

The authors would like to extend their appreciation to the Deanship of Scientific Research at King Saud University for funding this work through Research Group No. RG-1437-031.

Appendix A. Supplementary data

Supplementary data to this article can be found online at https://doi.org/10.1016/j.jksus.2019.11.040.

References

Abas, S.N.A., Ismail, M.H.S., Siajam, S.I., Kamal, M.L., 2015. Development of novel adsorbent-mangrove-alginate composite bead (MACB) for removal of Pb(II) from aqueous solution. J. Taiwan Inst. Chem. Eng. 50, 182–189.

Adetokun, A.A., Uba, S., Garba, Z.N., 2019. Optimization of adsorption of metal ions from a ternary aqueous solution with activated carbon from Acacia Senegal (L.) Willd pods using Central Composite Design. J. King Saud Univ.-Sci. 31, 1452–1462.

Ajmal, M., Rao, R.A.K., Ahmad, R., Khan, M.A., 2006. Adsorption studies on *Parthenium hysterophorous* weed: removal and recovery of Cd(II) from wastewater. J. Hazard. Mater. B135, 242–248.

Alakhras, F., 2019. Biosorption of Cd(II) ions from aqueous solution using chitosan-iso-vanillin as a low-cost sorbent: Equilibrium, kinetics, and thermodynamic studies. Arabian J. Sci. Eng. 44, 279–288.

Aldawsari, A., Khan, M.A., Hameed, B.H., et al., 2017. Mercerized mesoporous date pit activated carbon – A novel adsorbent to sequester potentially toxic divalent heavy metals from water. PLoS One 12, (9) e0184493.

Alqadami, A.A., Khan, M.A., Otero, M., et al., 2018a. A magnetic nanocomposite produced from camel bones for an efficient adsorption of toxic metals from water. J. Clean. Product. 178, 293–304.
Alqadami, A.A., Khan, M.A., Siddiqui, M.R., Alothman, Z.A., 2018b. Development of citric anhydride anchored mesoporous MOF through post synthesis modification to sequester potentially toxic lead (II) from water. Micro. Meso. Mater. 261, 198–206.
Alsohaimi, I.H., Wabaidur, S.M., Kumar, M., et al., 2015. Synthesis, characterization of PMDA/TMSPEDA hybrid nano-composite and its applications as an adsorbent for the removal of bivalent heavy metals ions. Chem. Eng. J. 270, 9–21.
Bhunia, P., Chatterjee, S., Rudra, P., De, S., 2018. Chelating polyacrylonitrile beads for removal of lead and cadmium from wastewater. Sep. Puri. Technol. 193, 202–213.
Bohli, T., Ouederni, A., Fiol, N., Villaescusa, I., 2015. Evaluation of an activated carbon from olive stones used as an adsorbent for heavy metal removal from aqueous phases. Comp. Rend. Chim. 18, 88–99.
Chen, K., He, J., Li, Y., et al., 2017. Removal of cadmium and lead ions from water by sulfonated magnetic nanoparticle adsorbents. J. Coll. Inter. Sci. 494, 307–316.
Farooghi, A., Sayadi, M.H., Rezaei, M.R., Allahresani, A., 2018. An efficient removal of lead from aqueous solutions using $FeNi_3@SiO_2$ magnetic nanocomposite. Surf. Interf. 10, 58–64.
Fatimah, Is, 2018. Preparation, characterization and physicochemical study of 3-aminopropyl trimethoxy silane-modified kaolinite for Pb(II) adsorption. J. King Saud Univ.– Sci. 30, 250–257.
Freundlich, H.M.F., 1906. Over the adsorption in solution. J. Phys. Chem. 57, 385–470.
Fu, R., Liu, Y., Lou, Z., et al., 2016. Adsorptive removal of Pb(II) by magnetic activated carbon incorporated with amino groups from aqueous solutions. J. Taiwan Inst. Chem. Eng. 62, 247–258.
Feng, Y., Wang, Y., Wang, Y., et al., 2017. Simple fabrication of easy handling millimeter-sized porous attapulgite/polymer beads for heavy metal removal. J. Coll. Interf. Sci. 502, 52–58.
Garmia, D., Zaghouane-Boudiaf, H., Ibbora, C.V., 2018. Preparation and characterization of new low cost adsorbent beads based on activated bentonite encapsulated with calcium alginate for removal of 2,4-dichlorophenol from aqueous medium. Inter. J. Bio. Macromol. 115, 257–265.
Ho, Y.S., McKay, G., 1998. Sorption of dye from aqueous solution by peat. Chem. Eng. J. 70, 115–124.
Ilton, E.S., Post, J.E., Heaney, P.J., et al., 2016. XPS determination of Mn oxidation states in Mn (hydr)oxides. Appl. Surf. Sci. 366, 475–485.
Jalees, M.I., Farooq, M.U., Basheer, S., Asghar, S., 2019. Removal of heavy metals from drinking water using chikni mitti (kaolinite). Arabian J. Sci. Eng. 44, 6351–6359.
Khan, M.A., Jung, W., Kwon, O.-H., et al., 2014. Sorption studies of manganese and cobalt from aqueous phase onto alginate beads and nano-graphite encapsulated alginate beads. J. Ind. Eng. Chem. 20, 4353–4362.
Khan, M.A., Alqadami, A.A., Otero, M., et al., 2019a. Heteroatom-doped magnetic hydrochar to remove post-transition and transition metals from water: Synthesis, characterization, and adsorption studies. Chemosphere 218, 1089–1099.
Khan, M.A., Otero, M., Kazi, M., et al., 2019b. Unary and binary adsorption studies of lead and malachite green onto a nanomagnetic copper ferrite/drumstick pod biomass composite. J. Hazard. Mater. 365, 759–770.
Langmuir, I., 1918. The adsorption of gases on plane surfaces of glass, mica and platinum. J. Am. Chem. Soc. 40, 1361–1403.
Lagergren, S., 1898. About the theory of so-called adsorption of soluble substances. K. Sven. Vetenskapsakad. Handl. 24, 1–39.
Lee, C., Jung, J., Pawar, R.R., et al., 2017. Arsenate and phosphate removal from water using Fe-sericite composite beads in batch and fixed-bed systems. J. Ind. Eng. Chem. 47, 375–383.
Luo, X., Yu, H., Xi, Y., et al., 2017. Selective removal Pb(II) ions form wastewater using Pb(II) ion-imprinted polymers with bi-component polymer brushes. RSC Adv. 7, 25811–25820.
Ngah, W.S.W., Fatinathan, S., 2010. Pb(II) biosorption using chitosan and chitosan derivatives beads: equilibrium, ion exchange and mechanism studies. J. Environ. Sci. 22, 338–346.
Pal, P., Pal, A., 2017. Enhanced Pb^{2+} removal by anionic surfactant bilayer anchored on chitosan bead surface. J. Mol. Liq. 248, 713–724.
Pawar, R.R., Lalhmunsiama, Kim, M., et al., 2018. Efficient removal of hazardous lead, cadmium, and arsenic from aqueous environment by iron oxide modified clay-activated carbon composite beads. Appl. Clay Sci. 162, 339–350.
Rauf, A., Arif, S., Shah, M.S., Lee, J.Y., et al., 2017. Non-stoichiometric SnS microspheres with highly enhanced photoreduction efficiency for Cr(VI) ions. RSC Adv. 7, 30533–30541.
Rao, R.A.K., Khan, M.A., Rehman, F., 2011. Batch and column studies for the removal of lead(II) ions from aqueous solution onto lignite. Ads. Sci. Technol. 29, 83–98.
Saha, A.K., Ray, S.D., 2013. Effect of cross-linked biodegradable polymers on sustained release of sodium diclofenac-loaded microspheres. Braz. J. Pharma. Sci. 49, 873–888.
Sahraei, R., Sekhavat, P.Z., Ghaemy, M., 2017. Novel magnetic bio-sorbent hydrogel beads based on modified gum tragacanth/graphene oxide: Removal of heavy metals and dyes from water. J. Clean. Prod. 142, 2973–2984.
Teoh, Y.P., Khan, M.A., Choong, T.S.Y., 2013. Kinetic and isotherm studies for lead adsorption from aqueous phase on carbon coated monolith. Chem. Eng. J. 217, 248–255.
Tran, H.V., Tran, L.D., Nguyen, T.N., 2010. Preparation of chitosan/magnetite composite beads and their application for removal of Pb(II) and Ni(II) from aqueous solution. Mater. Sci. Eng. C. 30, 304–310.
Voo, W.-P., Lee, B.-B., Idris, A., et al., 2015. Production of ultra-high concentration calcium alginate beads with prolonged dissolution profile. RSC Adv. 5, 36687–36695.
Wang, Y., Yao, W., Wang, Q., et al., 2016. Synthesis of phosphate-embedded calcium alginate beads for Pb(II) and Cd(II) sorption and immobilization in aqueous solutions. Trans. Nonferrous Met. Soc. China 26, 2230–2237.